Available online at www.sciencedirect.com
SCIENCE DIRECT®
Earth and Planetary Science Letters 239 (2005) 233–252
EPSL
www.elsevier.com/locate/epsl

Convective patterns under the Indo-Atlantic « box »

Anne Davaille [a,*], Eléonore Stutzmann [a], Graça Silveira [b,c], Jean Besse [a], Vincent Courtillot [a]

[a] Institut de Physique du Globe and CNRS, 4 Place Jussieu, 75252 Paris cedex 05, France
[b] Centro de Geofísica da Universidade de Lisboa Edifício C8, Campo Grande, 1749-016 LISBOA, Portugal
[c] Instituto Superior de Engengaria de Lisboa Avenida Conselheiro Emídio Navarro, 1949-014 LISBOA, Portugal

Received 4 January 2005; received in revised form 23 July 2005; accepted 27 July 2005
Available online 10 October 2005
Editor: S. King

Abstract

Using fluid mechanics, we reinterpret the mantle images obtained from global and regional tomography together with geochemical, geological and paleomagnetic observations, and attempt to unravel the pattern of convection in the Indo-Atlantic "box" and its temporal evolution over the last 260 Myr. The « box » presently contains a) a broad slow seismic anomaly at the CMB which has a shape similar to Pangea 250 Myr ago, and which divides into several branches higher in the lower mantle, b) a "superswell" centered on the western edge of South Africa, c) at least 6 "primary hotspots" with long tracks related to traps, and d) numerous smaller hotspots. In the last 260 Myr, this mantle box has undergone 10 trap events, 7 of them related to continental breakup. Several of these past events are spatially correlated with present-day seismic anomalies and/or upwellings. Laboratory experiments show that superswells, long-lived hotspot tracks and traps may represent three evolutionary stages of the same phenomenon, i.e. episodic destabilization of a hot, chemically heterogeneous thermal boundary layer, close to the bottom of the mantle. When scaled to the Earth's mantle, its recurrence time is on the order of 100–200 Myr. At any given time, the Indo-Atlantic box should contain 3 to 9 of these instabilities at different stages of their development, in agreement with observations. The return flow of the downwelling slabs, although confined to two main « boxes » (Indo-Atlantic and Pacific) by subduction zone geometry, may therefore not be passive, but rather take the form of active thermochemical instabilities.

Keywords: convection; mantle plumes; hotspots; traps; tomography

1. Introduction: the Indo-Atlantic « box »

A strong spherical harmonic degree two in geoid and seismic tomography suggest that the Earth's mantle is divided in two "boxes" by subducted plates [1], the Pacific box being isolated by its subduction belt [2]. The rest of the mantle constitutes the Indo-Atlantic box. Seismic data provide a present-day snapshot of mantle dynamics, but the two « boxes » and the subduction belt can be traced back at least 200 Myr [3]. The present-day Indo-Atlantic « box » comprises

* Corresponding author.
E-mail address: davaille@ipgp.jussieu.fr (A. Davaille).

0012-821X/$ - see front matter © 2005 Elsevier B.V. All rights reserved.
doi:10.1016/j.epsl.2005.07.024

the large East–West scar left by subduction of the Tethys. Its upper thermal boundary condition is complex: at least half of its surface is continental lithosphere which is thicker than oceanic lithosphere and more insulating [4]. The Atlantic and Indian oceans opened during the last 200 Myr and are still expanding (Fig. 1). Cells of large lengthscale surviving on long timescales are typical of plate tectonics [5] and form the longest possible wavelengths of mantle convection. We shall look at the dynamics of mantle convection on shorter time- and length-scales within the Indo-Atlantic region.

The mantle is cooled from above, and heated from within and below. The relative proportion of the two is still debated. If the mantle is still mainly heated from within, upwelling flow should be diffuse and passive, the bulk of the mantle rising gently as a response to sinking slabs. This dominant slab signal can explain most of the geoid [6], present and past plate motions [7], part of the history of uplift and subsidence of continents [8], and the strong degree 2 features in seismic images (e.g. [1,9]). However, anomalously large topography or bathymetry, such as the Polynesian [10] or African [11] superswells, are probably due to more localized deep active upwellings [12,13]. Moreover, tomographic images show that mantle seismic velocities are not uniform away from the slabs and that several slower 3D structures are present. Based on recent fluid mechanics results, we propose that such structures constitute evidence of convective upwelling instabilities, and therefore that the mantle is also significantly heated from below. We reinterpret global tomography images and geochemical, geological and paleomagnetic observations, and try to unravel the convective pattern in the Indo-Atlantic mantle and its evolution over the last 260 Myr.

2. Observations

2.1. Present-day surface observations

The Indo-Atlantic box is covered by 50% continents and 50% oceans comprising seven tectonic plates. Relative plate motions deform its top which is currently shortening along the Himalayan and Alpine convergence zones, while it is expanding at the Atlantic and Indian ridges. The box net expansion rate is 0.6 km^2/yr over the last 200 Myr.

"Hotspots" are defined as long-term sources of volcanism which seem relatively fixed compared to the plates [14]. The Indo-Atlantic box hosts about 25

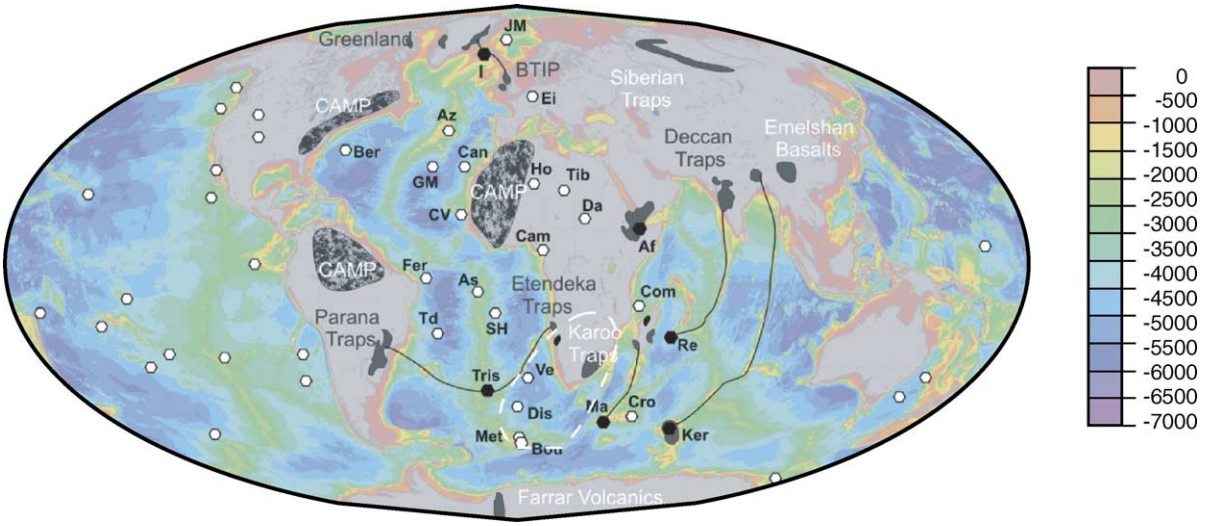

Fig. 1. Bathymetric map of the Indo-Atlantic box with active hotspots (black and white hexagons) and traps (shaded grey). The « primary » hotspots (black hexagons) are linked to their traps by a solid line. The African superswell area is enclosed in the white dashed line. JM : Jan Mayen; I : Iceland; Ei : Eifel; Az : Azores; Ber : Bermuda; GM : Great Meteor; Can :Canary; Ho : Hoggar; Tib : Tibesti; CV : Cape Verde; Da : Darfur; Af : Afar; Cam : Cameroon; Fer : Fernando; As : Ascension; Com : Comores; Td : Trinidad; SH : St Helena; Re : Reunion; Tris : Tristan; Ve : Vema; Dis : Discovery; Crz : Crozet; Met : Meteor; Bou : Bouvet; Ma : Marion; Ker : Kerguelen.

hotspots [15–18], mostly located NW of the African continent or near the Atlantic and West Indian ridges (Fig. 1); all are above or close to a mantle bottom slow seismic velocity area (Fig. 2). Six terminate long volcanic tracks which originated at large flood basalt events: Iceland, Tristan, Marion, Kerguelen, Réunion and Afar (Fig. 1). These "primary hotspots", may be due to impingement of mantle plumes under the lithosphere [18–20]. Petrological [21] and geophysical [16] studies suggest that hotspot material is 150 to 300 °C above normal mantle temperature. It also sometimes displays large isotopic ratios of He, Ne and Xe [22], a rare gas signature often interpreted as characteristic of a deeper, more primitive reservoir.

Nyblade and Robinson [11] noticed elevated topography in South Africa, which they linked to abnormal bathymetry in the nearby ocean; Gurnis and al [23] estimated residual topography and average uplift rate during the last 30 Myr to be 300–600 m and 5–30 m/Myr respectively. This "superswell" could be interpreted as active uplift in relation to a large buoyant structure within the lower mantle [13,23].

2.2. Seismic observations

Seismic tomographic models give an instantaneous image of the mantle. At the bottom of the lower mantle, all 1D-models, such as PREM [24], show a layer of lower seismic velocity gradient (D″). Superimposed, slower, large-scale velocity structures, as beneath South Africa or the Pacific, are robust global tomography features. Joint inversion of both P- and S-wave velocity constrains mantle temperature and composition. The resulting ratio $R = \mathrm{dlnVp}/\mathrm{dlnVs}$ reaches a maximum ~2.5 at the bottom of the South African mantle [25], which probably require compositional heterogeneities in addition to thermal effects [26]. Normal mode data (e.g. [27]) confirm this view.

Long-wavelength Vs models yield more uniform resolution throughout the mantle than high-resolution Vp models, which often lack coverage in the suboceanic mantle [28]. Therefore, Vs models are more appropriate to investigate the morphology and geometry of slow anomalies. Large scale structures (up to degree 6–8) are similar for all S-wave models but there are still differences in smaller wavelengths. We have compared three recent models, TXBW [29], SAW24B16 [30] and S20RTS [31]. These three models are derived from different observables, theories and model parameterizations (see supplementary material). Differences between them are useful to ascertain robust features. We show model TXBW in Fig. 2, and the other two as supplementary material.

Subductions are mostly located at the edges of the Indo-Atlantic box except for the Tethys subduction which extends eastward from Western Europe to the Pacific. At the mantle bottom, the three models present a broad slow anomaly (Fig. 2.1), covering about 27×10^6 km^2, with amplitudes between −0.5% and −3%. A small slow-velocity patch under Eurasia is isolated from the main slow area by the Tethys subduction. Although images are blurred, several extrema can be distinguished. Model TXBW (Fig. 2.1) shows four intensity extrema above the CMB located around A (64.5° E/46° S, East of Kerguelen), B (12° E/39° S, tip of African superswell below Atlantic Ocean), C (14° E/12° S under Guinea) and D (16.5° W/17° N, just East of Cape Verde). Their spacings range between 1600 and 3200 km at the CMB. In the other models, points ABCD are located close to extrema, although they may not coincide exactly. In all models, Afar, Réunion, Tristan da Cunha and Iceland are located near the edges of the broad slow zone, with either no slow anomaly or a faint one (Fig. 2.1).

In the bulk of the mantle, slow anomalies present complex 3D structures (Fig. 2). One of the most significant is located beneath the « superswell », extending under southern Africa and the southern Atlantic Ocean : close to B, the three models show anomalies slower than −1% to −2% from the CMB up to 2000 km-depth (Fig. 2.2 and 2.4), while further North–East under Africa, velocities slower than −0.5% to −1% are found from the CMB up to 1000–700 km-depth (Fig. 2.4). There is no evidence for slow upper mantle Vs in the whole superswell area. Analysis of differential travel times measured on a dense array in South Africa provide a sharper image of the strongest part of the anomaly [32–34]. It extends from the CMB to about 1500 km above, with a ~3% drop in Vs (Fig. 2.4). It appears to be a banana-shaped ridge, 1200 km-wide and 7000 km-long, from mid-Africa, where it strikes roughly northwest, to beyond the tip of South Africa where it bends toward the Indian ocean (area between white lines in Fig. 2.1). The combination of a) sharpness of the boundaries, b) broadness of the structure, and c)

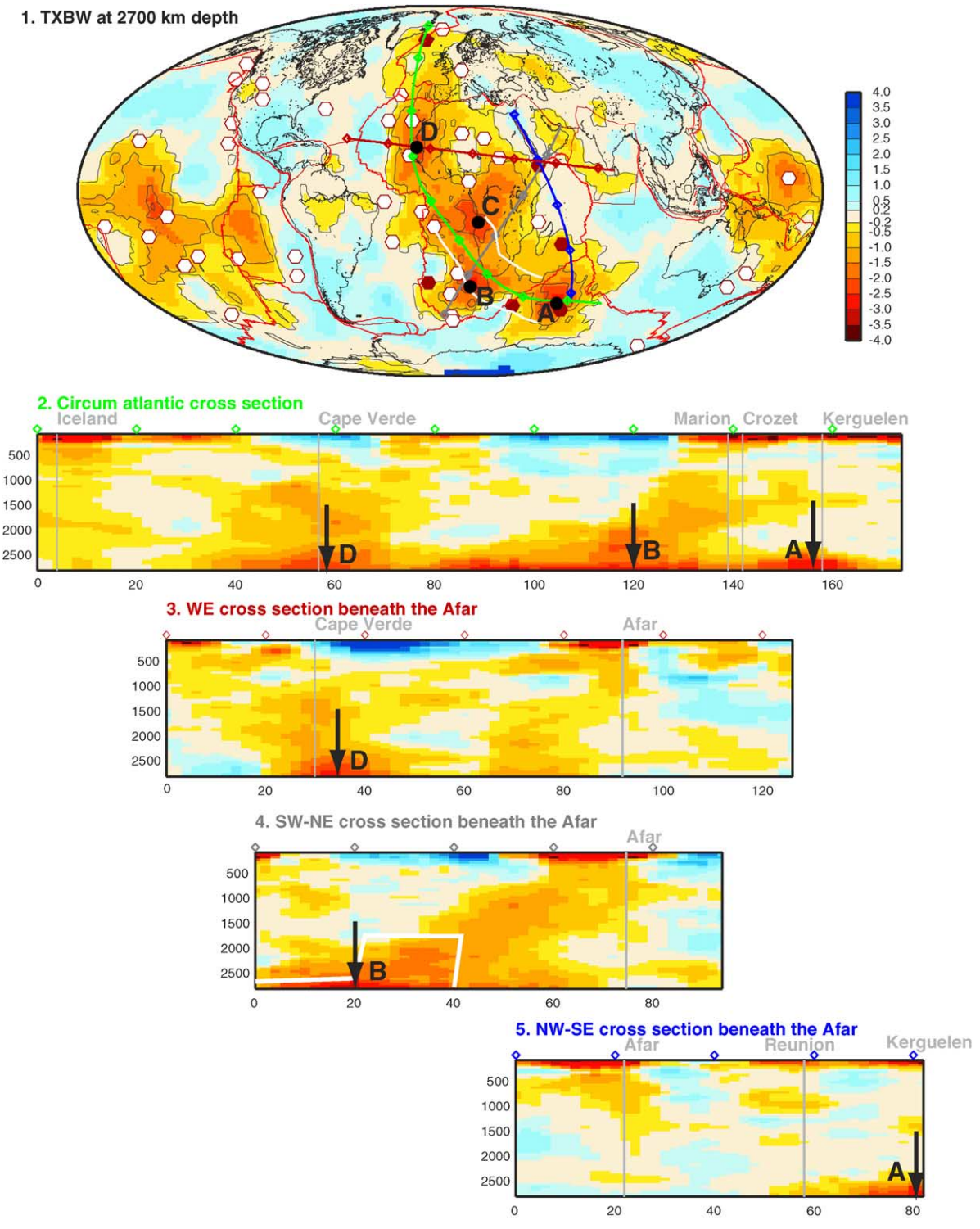
1. TXBW at 2700 km depth
D
C
B
A
4.0
3.5
3.0
2.5
2.0
1.5
1.0
0.5
0.2
-0.2
-0.5
-1.0
-1.5
-2.0
-2.5
-3.0
-3.5
-4.0
2. Circum atlantic cross section
Iceland
Cape Verde
Marion
Crozet
Kerguelen
500
1000
1500
2000
2500
0
20
40
60
80
100
120
140
160
D
B
A
3. WE cross section beneath the Afar
Cape Verde
Afar
500
1000
1500
2000
2500
0
20
40
60
80
100
120
D
4. SW-NE cross section beneath the Afar
Afar
500
1000
1500
2000
2500
0
20
40
60
80
B
5. NW-SE cross section beneath the Afar
Afar
Reunion
Kerguelen
500
1000
1500
2000
2500
0
20
40
60
80
A

much larger contrast in Vs than in Vp, suggests that this structure may have a different composition than the rest of the mantle. The circum-Atlantic cross-section (Fig. 2.2) further shows that it dips upwards towards the Marion and Crozet hotspots, reaching 800 km-depth in TXBW (and S20RTS, and 1500 km-depth in SAW24B16). The upper mantle beneath this area is very slow in all models. The Kerguelen hotspot is located above a strong slow velocity anomaly at the CMB and in the upper mantle, but the mantle in between does not display a continuous slow structure (Fig. 2.5).

In continuation with the banana-shaped structure, there is a 2000–4000 km-wide anomaly under Cape Verde (Fig. 2.2), rising in all models up to 1000–800 km-depth. The structure appears vertical and cylindrical (Fig. 2.2–3). The upper mantle above this area does not display clear systematics. Regional studies show large slow anomalies which do not seem to go deeper than 300 km beneath Azores and Cape Verde [35]. Further North, beneath Iceland, all three models show a strong anomaly (−3% to −2%) in the upper mantle, in agreement with regional studies (e.g. [36]). In the lower mantle, TXBW shows a weaker though significant slow anomaly (slower than 1%) down to the CMB, but no strong slow anomaly in D″ (Fig. 2.2), while SAW24B16 and S20RTS show only a weaker, patchy anomaly in the mid-lower mantle. Fig. 2.3 and 2.5 display a rather tubular slow anomaly beneath Afar from the surface down to at least 800–1000 km-depth, but no strong anomaly at the base of the mantle beneath it. Beneath the East African rift (Fig. 2.4), another strong slow anomaly, may be connected with Afar, occupies the upper mantle, as also observed in regional models [37]. Models S20RTS and TXBW further show a continuous slow region extending from the mantle bottom beneath South Africa to the upper mantle beneath the East-African rifts (Fig. 2.4). There is no systematic slow anomaly beneath Reunion, except close to the surface and near 1000 km depth (Fig. 2.5).

Montelli et al.'s [38] P-wave tomographic study focusses on the depth extent of slow anomalies directly beneath hotspots. In the lower mantle, these anomalies are rather weak (−0.3% to −0.5%). Slow anomalies of 200–400 km radius extend down to the CMB beneath Ascension/St. Helena, Azores and Canaries, down to 2350 km beneath Crozet, 1900 km beneath Cape Verde, Reunion and Seychelles, 1450 km beneath Afar, Bouvet, and Iceland. Resolution at the bottom of the mantle does not allow to follow them deeper. These seem to confirm the existence of deep-rooted hot anomalies beneath some hotspots, which could correspond to plume conduits. Tubular slow anomalies beneath Azores, Canaries and Cape Verde seem to merge below 1400 km-depth into a broader anomaly, and so do Kerguelen and Crozet below 2300 km-depth. Both wide anomalies were also imaged in previous models (e.g. Fig. 2).

In summary, continuous stratification is not found in the lower mantle. Instead, seismic data display slow anomalies with diverse morphologies. There seem to be several extrema just above the CMB, three large (~2000 km-wide) 3D slower structures extending from the CMB upwards to about 800 km-depth (under Cape Verde, South Africa, and Marion/Crozet), one 7000 km-long ridge-like structure at the mantle bottom under west and south Africa, prominent slow anomalies extending from the surface downwards at least to 700 km-depth under Iceland, Afar, the East-African rift, and Kerguelen, and several thinner tubular structures under some hotspots. However, slow conduits of diameter smaller than 200 km would not be detected.

2.3. Long-term history

The most recent supercontinental assemblage, Pangea (Fig. 3a), lasted at least from 330 Myr to around 200 Myr. Breakup of Pangea began with « re-opening » of the central Atlantic 180 Myr ago (Fig. 3b). Shortly thereafter, the southeastern part of Pangea started to disintegrate, with initial rifting ~180 Myr ago, forming a seaway between West and East Gondwana (Fig. 3b,c). 130 Myr ago, Australia–India–Antarctica separated from an African–South

Fig. 2. Cross-sections through model TXBW by Grand [29]. 1) maps at 2700 km depth. In black, the four extrema discussed in the text. In white, the banana-shape slow anomaly determined by Ni and Helmberger [34]. The radial cross-sections shown in 2)–5) are along the colored solid lines. 2) Circum-Atlantic cross-section; 3) Cape Verde to Afar cross-section; 4) South Africa to Afar cross-section; 5) Afar to Réunion to Kerguelen cross-section.

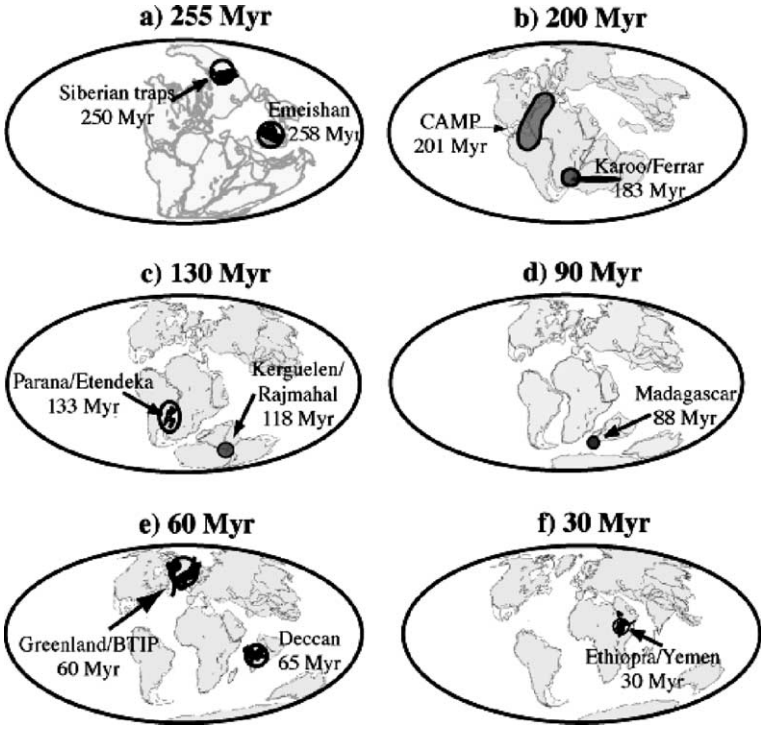

Fig. 3. Paleomagnetic reconstruction of the continents'position compared to the Earth's rotation axis. Plate reconstructions of main blocks from present to 200 Myr are derived from the apparent polar wandering paths and kinematics proposed in Besse and Courtillot [77]. The method was to transfer carefully selected paleomagnetic data available for the Eurasian, African, North American and Indian on a single plate, using high-quality recent models for the opening of the North and Central Atlantic and Indian Oceans. At the scale we are working on, reconstructions based on the 1991 paper are not as significantly different from a later model [78] that they can alter our present conclusions. Position of Asian central blocks are from Zhao et al. [79], Besse et al. [80] and Halim et al. [81], while Chinese blocks position are derived from Yang and Besse [82]. The 255 Myr reconstruction is derived from the A Pangea of Fluteau et al. [83]. The maps were finally created using the Paleomac software developed by Cogné [84].

American plate (Fig. 3c); India split from Antarctica–Australia at ~110 Myr. Australia and New Zealand separated from the Antarctic core, and Madagascar, then the Seychelles separated from India as it migrated northwards (Fig. 3c to e). On the Atlantic side, the opening of the South Atlantic started 130 Myr ago (Fig. 3c), and the North Atlantic 110 Myr ago, progressively dislodging Greenland, first from North America and then from Eurasia since 60 Myr ago (Fig. 3d to e). Since ~30 Myr, the morphology of the Atlantic and Indian oceans has remained stable, the most recent event being the opening of the Red Sea and Gulf of Aden (Fig. 3f).

Plate tectonic forces (slab-pull and back-arc effects) and very large trap events attributed to mantle upwellings have been invoked as causes of continental breakup. The Indo-Atlantic box recorded 10 trap events in the last 260 Myr, 7 related to continental breakup, and 6 located at the beginning of a hotspot track (Fig. 1). In each case, the main volcanic phase was short-lived (<1 Myr), extended over $2–5 \times 10^6$ km^2 and produced $1–10 \times 10^6$ km^3 of lava [39]. The Emeishan traps erupted 258 Myr ago on the western side of Tethys, close to the equator, whereas the Siberian traps erupted 250 Myr ago close to 70°N (Fig. 3a). Neither trap is linked to a track, nor to ocean opening. The 200 Myr-old Central Atlantic Magmatic Province (CAMP) intruded Northern and Central Brazil, part of the western African craton, Eastern North America and Southwesternmost Europe [40]; it is associated with Central Atlantic breakup (Fig. 3b) but not to any track. The Karoo, Ferrar and Tasman volcanics erupted 183 Myr ago, predating the breakup of East Gondwana [41]. Like CAMP, it displays an

elongate shape (Fig. 3b). Parana (South America) and Etendeka (Africa) are part of the same trap which erupted 133 Myr ago, foreboding opening of the South Atlantic (Fig. 3c). They are linked to Tristan da Cunha hotspot through two continuous volcanic tracks (Rio Grande Rise and Walvis ridge). The Kerguelen Plateau, the Rajmahal traps in India and the Bunbury basalts in western Australia were emplaced at 118 Myr, when India and Australia separated from Antarctica (Fig. 3d). The Rajmahal are linked to the present-day Kerguelen hotspot through the 90°E and Broken ridges. In that same area, the Madagascar traps (Fig. 3d), which are linked to the Marion hotspot by a track, erupted 88 Myr ago. Shortly after India separated from the Seychelles, the Deccan traps erupted 65 Myr ago (Fig. 3e). A continuous chain of volcanoes links the Deccan to the present day Réunion hotspot. The British Tertiary Igneous Province (BTIP) and the traps in Greenland were emplaced 61 Myr ago, when the North Atlantic ocean began to open (Fig. 3e). Both are linked by continuous volcanism to the present-day Iceland hotspot. Finally, the Afar hotspot is associated with the Ethiopian and Yemen traps (Fig. 3d) emplaced 30 Myr ago.

In the Siberian traps, mantle melting has been estimated between 10–30% and started between 120 and 145 km-depth from a material around 1550 °C, i.e. around 250 °C hotter than normal MORBs material [42]. Similarly, BTIP material was estimated at 1550–1650 °C [43], while Etendeka material may have been as hot as 1700 °C, i.e. 400 °C hotter than ambient mantle [44], and even hotter than present-day hotspot material. High-resolution regional tomography under the Parana traps images both a Vp and Vs slow anomaly extending down to about 900 km depth [45]. A slow Vp anomaly from 80 to 400 km is reported under the Deccan [46]. Using S receiver functions, Vinnik et Farra [47] imaged slow-velocity bodies at 480 km-depth below the Afar, 350 km-depth below the Siberian and Karoo traps, for which they suggest a chemical origin. Traps therefore seem associated with hot material and slow seismic roots, possibly chemically differentiated from the mantle.

In Fig. 4, we compare (a) the paleomagnetic reconstruction of Pangea with the present distribution of seismic velocity anomalies at the bottom of the mantle, and (b) the locations of flood-basalts at the time of eruption as determined from plate kinematics and paleomagnetism, to the present-day distribution of continents and tomographic anomalies at the base of the mantle. Underdetermination of longitude due to axial symmetry of the Earth's magnetic field is an important limitation. However, since Africa is bounded by spreading zones and may have experienced only minor longitudinal motion, Burke and Torsvik [48] proposed a paleomagnetic reconstruction minimizing longitudinal motion of Africa. The result show only minor differences with respect to hotspot-based reconstructions for 0–130 Myr. We follow the same approach for our Pangea reconstruction, as well as for past trap reconstructions. Some striking features are worth mentionning: 1) The contour of the present-day seismic low-velocity anomaly at the base of the Indo-Atlantic mantle follows closely the shape of the core of Pangea at 250 Myr (Fig. 4a, [49]). 2) The original locations of the traps are along the edges or within the present-day seismic low velocity anomaly imaged above the CMB (Fig. 4b, [48]). 3) Traps avoid subduction zones: there are none along the Africa–Eurasia and India–Asia collisions. 4) Projected at the CMB, the distance between traps is typically 2000–3000 km, except for Madagascar and Kerguelen/Rajmahal. There have been no traps under Central Africa. 5) The Karoo erupted within what is now the oceanic part of the African Superwell, underneath the Bouvet hotspot [41]. The CAMP erupted in the central East Atlantic region, close to Cape Verde [50].

3. Convective instabilities in the mantle

Our image of mantle upwellings is still dominated by plumes issued from a steady point source of buoyancy [51,52]. In a fluid whose viscosity depends strongly on temperature, this set-up generates steady « cavity plumes » with large heads and thin trailing conduits [53]. Traps would be produced by impingement under the lithosphere of 1000 km heads and long-lived hot spot tracks by impingement of 100 km conduits [19,20]. However, it is not easy to produce steady narrow plumes from a surface heated from below [54]. Moreover, this model only accounts for the 6 « primary hotspots », while the Indo-Atlantic box contains about

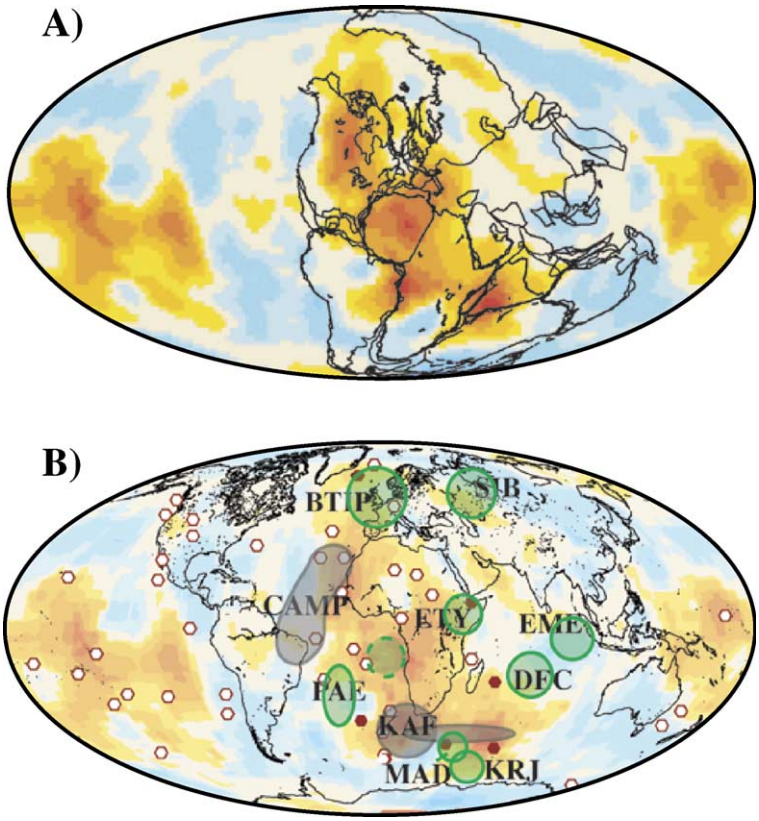

Fig. 4. a) Pangea 250 Myr ago on Grand's present-day seismic tomography model at the CMB. b) Traps locations at the time they were emitted (reconstructed with paleomagnetic data) projected on Grand's present-day seismic tomography model at the CMB. The dash circled represents the location of the event which produced 145 Myr ago rifting inWest and Central Africa, and which may associated with the St Helena hotspot track (e.g. [50]).

25 hotspots of various types. Neither does it explain a) the existence of « superswells », b) the three broad low seismic velocity anomalies, c) the banana-shape ridge imaged in the lower mantle, or d) the existence of traps not linked to long-lived volcanic tracks. A broad terminology involving « superplumes », « mega-plumes », « plume clusters », « diapirs », « cavity plumes », « domes », « piles », « ridges » or « anchored plumes » has been developed in order to differentiate observations made either in seismic images or in convection experiments from « the » mantle plume model. In the following, we review briefly the physics which lies behind these terms.

3.1. Purely thermal instabilities in the deep mantle

In a mantle layer (partly) heated from below, convection intensity is determined by the global Rayleigh number, which is the ratio of the driving thermal buoyancy forces to the resisting effects of thermal diffusion and viscous dissipation, $Ra = \alpha g \Delta T H^3 / \kappa \nu$, where H is the fluid depth, ΔT the temperature difference across it, g the gravitational acceleration, α the thermal expansivity, κ the thermal diffusivity and ν the kinematic viscosity. Thermal plumes (Fig. 5a) develop from the hot bottom thermal boundary layer (TBL) when Ra exceeds 10^6. For Earth-like average

Fig. 5. Regimes of thermochemical convection as a function of Rayleigh number and buoyancy number. Black circles: whole-layer convection (open circles for experiments close to marginal stability.), '+': stratified convection and anchored plumes with a deformed interface (light shaded area.), 'x': stratified convection with a flat interface, '*': stratified convection and anchored plumes with a non-convecting thinner layer. Laboratory experiments are shown in red [85], dark blue [86], yellow [69] and black [57,59,61,62,67]. Numerical calculations are shown in grey [87], light blue [66], brown [88,89], purple [90], green [91] and pink [92].

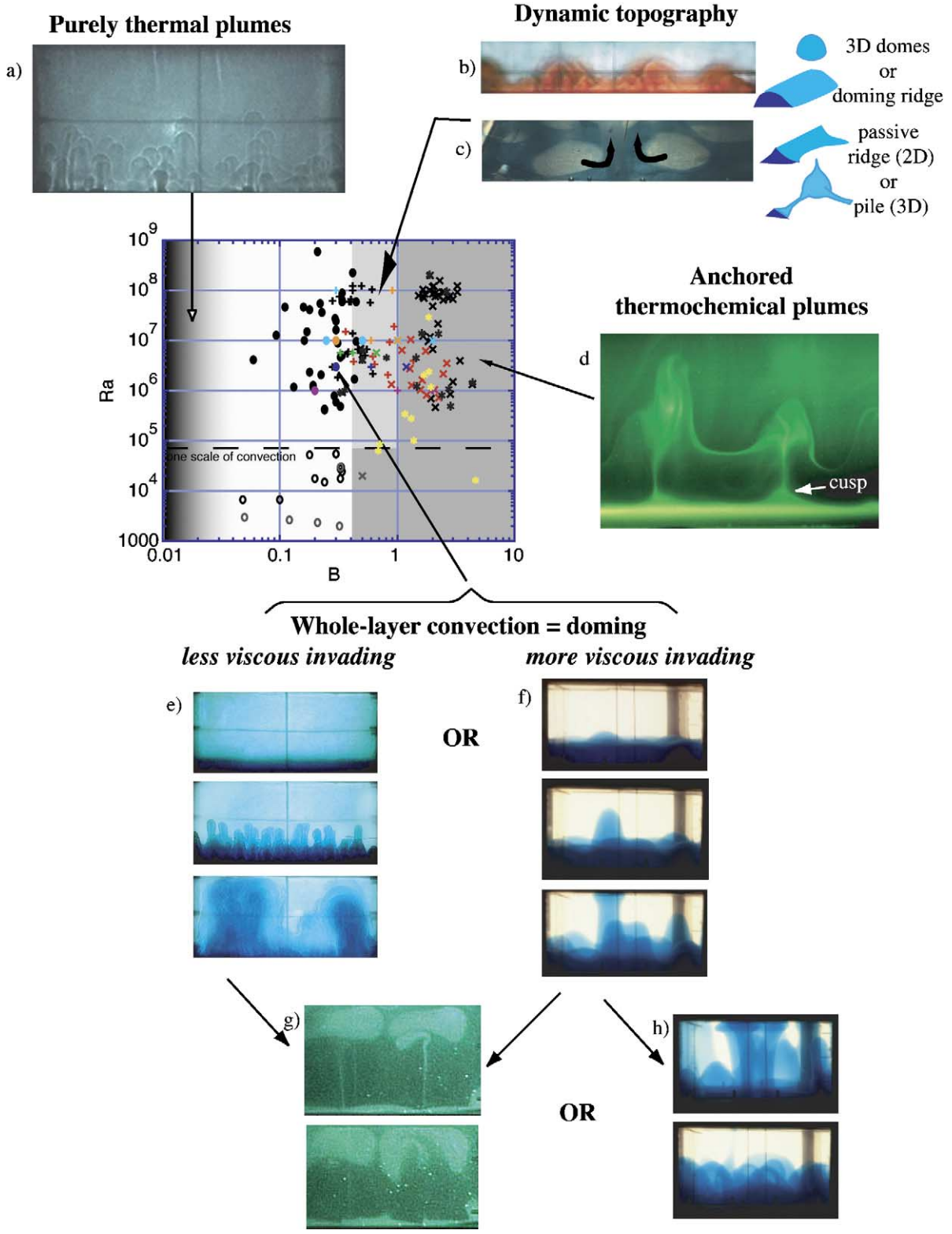
Purely thermal plumes
a)
Dynamic topography
b)
c)
3D domes
or
doming ridge
passive
ridge (2D)
or
pile (3D)
Ra
B
one scale of convection
Anchored
thermochemical plumes
d
cusp
Whole-layer convection = doming
less viscous invading
more viscous invading
e)
OR
f)
g)
h)
OR

viscosity (10^{22} Pa s, [6]), this is fullfilled if the mantle layer involved in convection exceeds 2000 km. Therefore, convective instabilities developing from the bottom mantle TBL above the CMB, often assimilated with D″, should be plumes. However, in a chemically homogeneous mantle, hot thermal plumes would present typical diameters less than 100–300 km, with head diameters only less than twice their stem radius (Fig. 5a), and a spacing from 100 to 850 km at the CMB [55]. The typical temperature anomalies of these purely thermal plumes would range between 50 and 200 °C, less than the 300 °C anomaly required to explain hotspot petrological data [21], and much smaller than the 1000 °C temperature difference across the D″ layer [56]. Moreover the typical lifetime of hotspots produced by such plumes would be under 40–50 Myr [57], too short to explain long volcanic tracks (up to 130 Myr, see [39]). So, if hotspots and traps are due to convective instabilities from D″, we need mechanisms to 1) stabilize part of D″, 2) produce larger plume heads with temperature anomalies not greater than 300–500 °C, and 3) anchor plume stems to generate long-lived volcanic tracks.

3.2. Zoology of upwellings in an heterogeneous mantle

Since both geochemical and seismological observations show that the mantle is heterogeneous in composition and density, studies of convection in a heterogeneous fluid have been performed, starting with a mantle initially stratified in density, and with viscosity depending on composition and/or temperature. The interaction between compositional heterogeneities and thermal convection generates a large diversity of upwellings. For Rayleigh numbers greater than 10^5, two scales of convection coexist, with purely thermal plumes (made of a single fluid) developing in each layer, and thermochemical instabilities (made of a mixture of the two fluids) developing in the whole system. Fig. 5 and Table 1 summarize the different regimes observed in the laboratory and numerical experiments. The key parameter is $B=(\Delta\rho_x/\rho)/\alpha\Delta T$, the buoyancy ratio of the stabilizing chemical density anomaly $\Delta\rho_x$ to the destabilizing thermal density anomaly [58,59]. For B smaller than ~0.03, density heterogeneities are so weak that they have no influence on the development of thermal convection, and the plumes have the same characteristics as already described in the previous section (Fig. 5a). For $0.03<B<B_c$~0.4, thermal effects can overcome the stable compositional stratification and convection develops over the whole layer, generating domes. Their temperature anomaly is mostly the slave of the compositional anomaly. Their direction of spouting and morphology depend on the layer depth ratio a and the effective viscosity ratio γ between the invading hot fluid and the upper fluid (Table 1), while their episodicity, diameter, wavelength, and velocity are mainly controlled by the more viscous layer [51,52,60,61]. For $B>B_c$, thermal effects can no more balance stable compositional stratification, and convection remains stratified, developing both above and below a more or less deformed interface, and producing anchored plumes. The whole spectrum of regimes can be obtained for density anomalies ranging from 0% to 2% [59], which is quite small. In the mantle, compositional heterogeneities could be created by slab remnants, delaminated continental material, relics of a primitive mantle, enriched for example in iron, or chemical reactions or infiltration from the core. Given these different processes, it seems reasonable to expect density anomalies of different magnitudes and sizes at different locations at the bottom of the Earth's mantle. We therefore expect simultaneous observation of different upwelling morphologies [59], among those displayed in Fig. 5, and different sequences of events (Fig. 7).

3.2.1. Large scale 3D seismic heterogeneities and superswells

Doming developing either in the whole-layer convection regime ($B<0.4$) or in the dynamic topography regime ($0.4<B<1$) would produce 3D low-velocity anomalies which could reach 2000 km- diameter (Fig. 5). While rising through the mantle, the domes would push the mantle upper boundary upwards, and therefore could generate « superswells » (Fig. 7A.1–2 and C.1–2). Domes would develop only in the mantle lower part (Fig. 5b,c) for $B>0.4$, but over the whole mantle for $B<0.4$ (Table 1, Fig. 5e–h). In the latter case, 300–500 °C thermal anomalies could be produced by 0.3–0.6% compositional density heterogeneities [62]. If viscosity depends only on temperature, this leads to domes 10–3000 timesless viscous than the bulk mantle : large cavity plumes (or

Table 1
Convective regime and upwellings morphology as a function of B, viscosity ratio γ, layer depth ratio a and internal Rayleigh number of the denser bottom layer Ra_d

B	Regim	$\gamma = \eta_d / \eta_m$	Ra_d	$a = h_d/H$	Upwellings morphology	Fig.	References
< 0.03	**1-layer**				**Thermal plumes** with no big head	5a	
0.03<B<B_c~0.4	**Whole-layer**				Active domes and passive ridges		[86, 61–62]
			< Ra_c ~1000		Passive **ridges** = return flow to downwellings	5c	
		< 1	>Ra_c	$a < a_c$ $a_c=1/(1+\gamma^{-1/3})$	Active hot upwellings **-Cavity plumes** (or « mega-plumes ») through collection of small thermal instabilities -detach from hot bottom boundary (HBB)	5e 5g	
			>Ra_c	$a > a_c$	Passive **ridges** =return flow to cold more viscous downwellings	5c	
		>1	> Ra_c		-Active hot **diapirs** detach from HBB if a<0.3 and B< 0.2 continuous fingers from HBB otherwise **-Secondary plumes** on top of domes	5f 5g 5h	
		1/5<γ < 5			**Overturning** = immediate stirring after first instabilities		[86]
		γ < 1/5 or γ >5			**Pulsations** = two layers retain their identity for several doming cycles	5f+5h	[59, 61–62]
> B_c	**2-layers**				**-Stratified** convection above and below interface **-Anchored** hot **thermochemical plumes** arise from TBL at the interface. No big head.	5b–d 5d	[85, 58, 67] [66, 57, 67, 59, 69]
B>1	Nearly flat interface				Thermochemical plumes in upper layer		[58,67]
B_c<B<1	**Dynamic topography**				Dynamic topography does not reach the upper boundary	5b–c	[66,61, 92]
		<1			Passive **ridges** (2D) or **piles** (3D) formed in response to cold viscous downwellings	5c	
		>1	<Ra_c		Passive **ridges** (2D) or **piles** (3D)	5c	
			Ra_c<Ra_d<10^4		Upwelling **ridges**	5b	
			>10^4		Upwelling **domes**, or **superplumes**	5b	

For depth- or temperature-dependent properties, the viscosities are taken at the averaged temperature of each layer, and α is taken at the interface [59,62]. We focuss on high global Ra (>10^6). Note that if Ra_d<Ra_c, the denser layer cannot convect on his own.

Thompson and Tackley's « mega-plumes » [63]) would therefore develop (Fig. 5e) and invade the more viscous bulk mantle if the thickness of the initial denser less viscous layer from which they are issued is less than 700–200 km (Table 1). This is the only case in which upwellings with big heads can be generated (Figs. 5g and 7A.3). However, the thin conduit would rapidly disappear, and the instability would be cut off from the mantle base (Figs. 5g and 7C.3).

3.2.2. Traps without tracks

Upon reaching the lithosphere, a dome would spread (Fig. 7C.3), melt, generating traps, and finally cool down. The dome material which has not melted would subsequently cool and fall back down. A volcanic track is not expected to follow the trap event (Fig. 7C.4).

3.2.3. Tracks without traps

Tracks without traps imply plumes with no big heads, i.e. purely thermal instabilities (Fig. 5a, $B<0.03$) or anchored thermochemical plumes ($B>0.4$, Table 1). In the latter case, convection remains stratified, a TBL develops at the interface and plumes develop from it in the upper layer. Their thermal anomaly scales with the temperature difference across the unstable part of the TBL above the interface [64–66]. As in the purely thermal case, they do not present a big head. While rising, these plumes entrain a thin film of the denser bottom layer by viscous coupling and locally deform the interface into cusps (Fig. 5d, [67]). The interfacial topography act to further anchor the plumes [68,57,59,69], which persist until the chemical stratification disappears through entrainment. Anchored plumes in the mantle would develop for chemical density contrast within D″ greater than 0.6%. They could survive hundreds of millions of years, depending on the size and magnitude of the chemical heterogeneity on which they are anchored, producing long-lived and relatively fixed hotspots on the lithosphere, but no traps.

3.2.4. Phase transition filter and secondary hotspots

Numerical studies show that the phase transition at 660 km depth is not sufficient to impede convection, but probably delays passage of convective features [70,71]. In the case of thermochemical features, they could pond under the transition zone (Fig. 7B.1). During this time, secondary plumes could be generated from the top of the hot dome (Fig. 7B.1). If the delay induced by the phase transition is too long, the thermochemical dome would lose its thermal buoyancy [62], become denser again and fall back (Fig. 7B.2). If the hot dome finally breaks through the phase transition, it would rapidly reach the lithosphere and produce traps (Fig. 7A.3 and C.3). The unmelted dome material would subsequently cool, fall back down and a new doming event could develop.

3.2.5. Episodicity

The « doming » regime, although chaotic in the sense that the location of the next instability cannot be exactly predicted, is episodic within an area scaling as the square of the spacing between two domes. For lower mantle viscosities between 4×10^{21} and 10^{22} Pa s [6], recurrence times range between 100 and 180 Myr (Fig. 6a).

3.2.6. Primary hotspots

Weak stratification could produce traps (big cavity plume head) without a long-lived volcanic track (conduit) while strong stratification would produce a long-lived track (anchored plume) without traps (Table 1). To produce a primary hotspot with traps at the beginning of a long-lived volcanic track, the bottom of the mantle probably needs to have continuous, slowly varying density stratification (Fig. 7A). The lighter part of the heterogeneous TBL (where $B<0.4$) would then become unstable (Fig. 7A.1) and rise through the mantle (Fig. 7A.2). The upwelling flow would cause the mantle upper boundary to swell, and could create a "superswell". Then the instability would reach the lithosphere, producing a large trap event at the surface (Fig. 7A.3). Meanwhile, the upwelling flow would have deformed the denser part of the TBL (where $B>0.4$), anchoring further the plume [68,57,59,69]. This would ensure a long-lived conduit and therefore a long-lived volcanic track (Fig. 7A.4–A.5), while the traps are carried away by plate motion. The volcanic track would end with the end of the plume conduit.

3.3. Plate tectonics, subduction and insulating continents

Convection with plate tectonics is characterized by cells with large aspect ratios, very localized weak

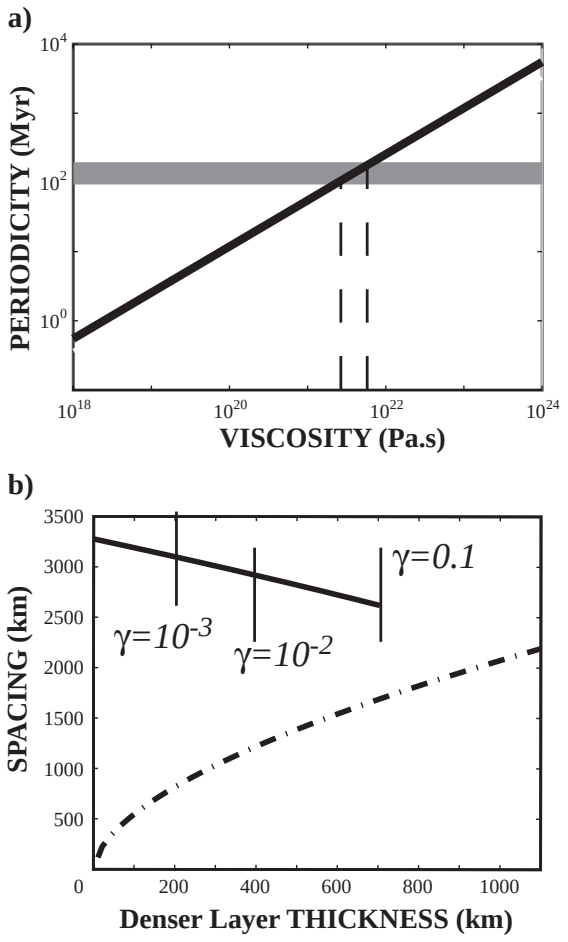

Fig. 6. a) Doming recurrence time as a function of the upper layer, i.e. bulk mantle, viscosity. The thickness of the black line takes into account the uncertainties on the periodicity introduced by the different mechanical boundary conditions between the mantle (free slip) and the laboratory experiments (no slip). See [62] for more details. b) Spacing between domes as a function of the denser layer thickness. Dash-dotted line, more viscous diapirs; solid line, less viscous cavity plumes heads. The latter can develop only if the hot less viscous layer is thinner than $h_c = H/(1+\gamma^{-1/3})$ [62]. The solid ticks mark the maximum possible thickness h_c for a given viscosity ratio. The spacing has been calculated using the experimental scaling laws, i.e. with no-slip conditions and cartesian geometry. We therefore expect the trends to be robust but the exact spacing values could be off by a factor of two, compared to a free slip, spherical mantle. McNamara and Zhong [92] recently performed a serie of numerical experiments in the slightly different « dynamic topography » regime, using a spherical domain with free slip outer boundary conditions. The spacings which they reported are indeed comparable to our experimental results, but a similar study should be run for the doming regime.

zones, and strong plates (see [5], for a recent review). On Earth, it is responsible for the degree-two pattern in the geoid and in the tomographic images, where the cold subducted material can be traced down to the CMB (e.g. [2,29]). In presence of such large scale circulation, laboratory and numerical experiments [72–75] show that hot instabilities cannot develop directly underneath the downwelling flow, which impedes growth of the hot TBL. Instead, the instabilities arise away from the downwelling. Then, depending on the strength of the large-scale flow, they are either deflected, or carried away and focussed in a single upwelling. This could explain plume clustering away from subduction zones [55,74] and along mid-ocean ridges [e.g. [73]], and, given the geometry of subduction zones, the confinement of present-day mantle upwellings into two « boxes ».

The Indo-Atlantic box also contains continents which do not subduct. Hence, when they are large enough (typically more than twice the mantle depth), they shield part of their underlying mantle from subduction (e.g. [49,4]), which promotes hot instabilities. Besides, continents are insulating and heat flow beneath them is significantly lower than under oceans. Continental lithosphere is also thicker than oceanic lithosphere. Hence, continents induce a lateral heterogeneity both in the mechanical and thermal conditions at the upper boundary of the mantle. This lateral heterogeneity may generate convective cold downwellings along the edges of continents. It has been proposed that such « edge-driven » convection could be confined to the upper mantle and could produce hot upwellings as return flows (e.g. [76]).

4. Temporal evolution of Indo-Atlantic convective motions in the last 260 Myr

We next use spacing and morphology of present-day seismic anomalies, together with temporal sequences of traps, and existence of superswells and some long-lived volcanic tracks, to infer the temporal evolution of convection and compositional heterogeneities in the Indo-Atlantic box. Our lack of knowledge of mineral physics limits what can be directly inferred from tomography. We therefore take the simplest view and interpret slow Vs areas as hotter, and possibly chemically heterogeneous, mantle.

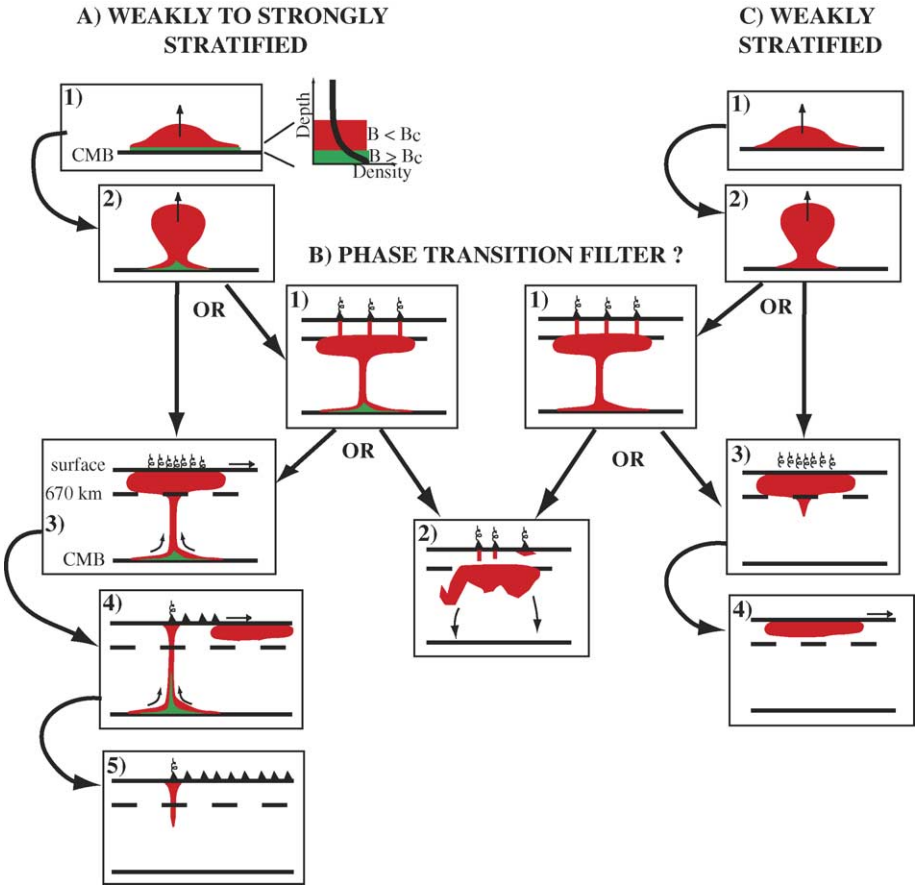

Fig. 7. Different scenarios for mantle upwellings and formation of large extent seismic low-velocity anomalies, superswells, traps, and long-lived volcanic tracks. See text for detailed explanations.

4.1. Pattern at a given time

The shape and location of the broad slow seismic velocity anomaly ($\leq -0.5\%$) at the bottom of the mantle are close to those of Pangea 250 Myr ago (Fig. 4). This is consistent with Pangea shielding the mantle from subduction and subduction zones being located on its outer edges. The slow seismic anomaly is not uniform throughout the box, but presents several 3D features (Section 2, and Fig. 2). Given their morphology, it is tempting to identify these with thermochemical instabilities, as described in Section 3. The six primary hotspots, as well as the three present-day cylindrical seismic heterogeneities (under Cape Verde, Marion/Crozet, and South Africa) would have involved the formation of a large cavity plume head (Fig. 5e). This would imply less viscous heterogeneities with density anomalies of compositional origin from 0.1 to 0.6%, and an instability spacing at the CMB from 1800 to 3500 km (Fig. 6b). Each instability would therefore drain a surface of 3 to 12×10^6 km^2. Since the area of slower and hotter material is currently 27×10^6 km^2 at the CMB, we expect 3 to 9 instabilities at different stages of their development.

Fig. 8. Fluid mechanics interpretation of Grand's tomographic model. 1) Zones of influence of thermochemical instabilities, represented by disks of 2000 and 3500 km-diameter (centered on A, B, C, D, Afar, Reunion, Iceland), are superimposed on Grand's tomographic model at 2700 km-depth. 2) Circum-Atlantic cross-section; 3) Cape Verde to Afar cross-section; 4) South Africa to Afar cross-section; 5) Afar to Réunion to Kerguelen cross-section. In red are the instabilities containing weakly heterogeneous fluid ($B < 0.4$), and in green the strongly heterogeneous fluid ($B > 0.4$).

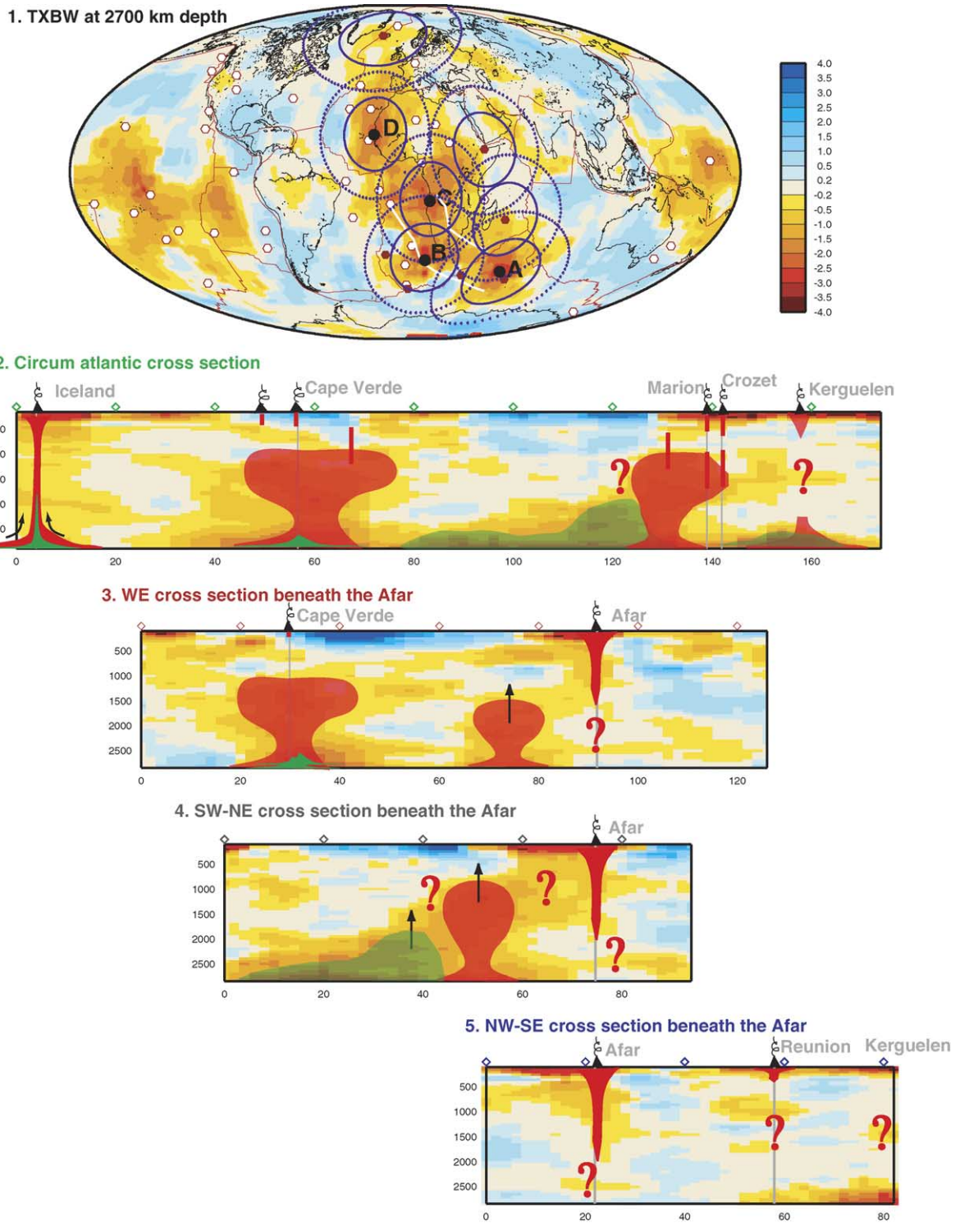
1. TXBW at 2700 km depth
D
C
B
A
4.0
3.5
3.0
2.5
2.0
1.5
1.0
0.5
0.2
-0.2
-0.5
-1.0
-1.5
-2.0
-2.5
-3.0
-3.5
-4.0
2. Circum atlantic cross section
Iceland
Cape Verde
Marion
Crozet
Kerguelen
500
1000
1500
2000
2500
0
20
40
60
80
100
120
140
160
3. WE cross section beneath the Afar
Cape Verde
Afar
4. SW-NE cross section beneath the Afar
Afar
5. NW-SE cross section beneath the Afar
Afar
Reunion
Kerguelen

In this framework, we interpret seismic images as showing at least 7 instabilities (Fig. 8): a) a large dome originating close to D at the CMB and ponding at the transition zone, wherefrom upper mantle secondary plumes produce the present-day Cape Verde, Canaries, Great Meteor and Azores hotspots (Fig. 7B.1 or B.2); another similar dome under Marion and Crozet hotpsots; b) a large upwelling rising below South Africa, but which has not yet reached the upper mantle (Fig. 7A.2 or C.2); c) four primary plumes beneath Iceland, Afar, Kerguelen and Réunion (Fig. 7A). According to Fig. 8, these plumes could originate deep in the lower mantle, even if present-day pictures do not provide clear evidence of a physical link with the deep mantle. In the case of Kerguelen and Iceland, where slow seismic anomalies exist at the CMB, this could be due to lack of resolution of tomographic models; a recent extension of the finite-frequency tomography of Montelli et al. [38] to S waves indeed seems to image a conduit in the lower mantle under the Icelandic plume (Montelli, pers. comm., 2004), confirming Grand's result (Fig. 2.2). The absence of slow anomalies at the CMB below Réunion and Afar could indicate that those plumes have exhausted all the material of the TBL in those areas and therefore are dying (Fig. 7A.5). Similarly, Tristan, which is not associated with any clear slow anomaly, could be in the last stages of its activity. The existence of anchored plumes implies density anomalies greater than 0.6% at the bottom of D″.

The Indo-Atlantic mantle also contains a longer-lived feature: as already noted by Ni and Helmberger [34], the morphology of the banana-shaped ridge at the bottom of the mantle compares well with the case of dynamic topography (Fig. 5b). The top of the seismic anomaly resembles a dome (Fig. 2.4) and the uplift of South Africa, may correspond to an active more viscous denser lower layer. This implies that $B_c \leq B \leq 1$, i.e. lower material 0.6% to 1.5% intrinsically denser than normal mantle. Since the shape of the doming ridge is elongated, its internal Rayleigh number is low, between 10^3 and 10^4 (Table 1). This implies that the viscosity of the denser ridge material ranges between 10^{23} and 3×10^{24} Pa.s. This might be remnants of primitive mantle [34], compatible with fluid mechanics which indicate that the dynamic topography regime could survive in the Earth for billions of years [59,62]. On the other hand, it might also be remnants of dehydrated slab material, in which case, we could be witnessing the building of a new mantle reservoir, whose size might provide constraints on past subduction rates.

We interpret the continuous slow structure from the bottom of the mantle beneath South Africa to the surface below Afar (Fig. 8.4) as a composite of at least three instabilities at different stages of their evolution. Material erupting at Afar cannot come from under South Africa, because its trajectory tilt, greater than 30°, is too big to be stable [51,52]. Moreover, the multiple instabilities interpretation is in better agreement with the events chronology: the Ethiopian traps erupted 30 Myr ago, while South Africa uplift started only 30 Myr ago and continues [23]. In the sequence of events producing a primary plume (Fig. 7), uplift would predate the trap event. So a common source for Afar and the South African superswell is ruled out.

4.2. Temporal evolution

The recurrence time between instabilities at a given location is 100–200 Myr for reasonable lower mantle viscosities (Fig. 6a). There are two places where such a succession may be observed. The African Superswell started to rise 30 Myr ago [23] where Karoo traps erupted 183 Myr ago (Fig. 4b). The hotspots of the Eastern central Atlantic ocean have been active in the last 40 Myr in the same area where part of CAMP erupted 200 Myr ago. There is an interval ~150 Myr between the two pairs of magmatic events. These could be attributed to thermochemical instabilities if the viscosity of the bulk lower mantle is between 5×10^{21} and 10^{22} Pa s (Fig. 6a), in agreement with independent estimates (e.g. [6]). The domes below Cape Verde and South Africa may be rebirths of CAMP and Karoo. Given its huge extent, the CAMP event could even have formed from two thermochemical instabilities. If the Emeishan, Siberia, CAMP and Karoo-Ferrar traps formed from weak density anomalies ($B < 0.4$, i.e. $\Delta\rho_x/\rho < 0.6\%$), they would rapidly have become exhausted, which might explain why these traps were not followed by long-lived volcanic tracks. According to Fig. 4b and the framework which we develop, some events are missing or have not been recorded by a large trap. One such event could have

produced rifting in West and Central Africa 145 Myr ago, associated with a large plume head and the St Helena hotspot track [50]. In this case, the continental lithosphere may have been too thick for the plume to pierce it and generate traps.

There is no trap in the vicinity of the Africa–Eurasia and India–Asia collisions, which represent the most recent stages of the Tethyan subduction (Fig. 4b). This is consistent with the necessity for hot instabilities to develop away from downwellings. This might alternatively explain why no rebirth of the Siberian and Emeishan instabilities has been observed yet despite the 250 Myr time lapse: although both areas at the CMB correspond to slower (and therefore probably hotter) material (especially under the Siberian traps), they are also now close to cold subducting slabs.

5. Conclusions

Return flow of downwelling slabs, although confined by subduction zone geometry, is not passive and may take the form of active thermochemical instabilities. Even though they are not strong enough to impede whole mantle convection, density heterogeneities less than 2% may greatly modify the morphology and characteristics of mantle upwellings. Given the diversity of sources of compositional heterogeneity at play in the mantle, it is not unreasonable to expect the simultaneous generation of different types of upwellings. In this framework, three-dimensional slow seismic velocity anomalies, superswells, traps and primary hotspots can be interpreted as representing different stages of evolution of thermochemical instabilities generated in the deep mantle.

The overall shape and location of the broad slow anomaly at the bottom of the mantle are similar to those of Pangea 250–200 Myr ago, suggesting that the supercontinent acted as a shield for the mantle beneath it. The broad slow anomaly is not uniform and we observe three domes which rise upward from it. Beneath the equatorial Atlantic and southwest Indian oceans, the domes pond under the transition zone: above, we observe secondary hotspots such as Cape Verde, Canaries, Great Meteor and Azores in the Atlantic Ocean and Marion and Crozet in the Indian Ocean. Beneath South Africa, another large upwelling has not yet reached the upper mantle, and a ridge-like structure, probably denser and more viscous, domes in the bottom of the mantle. There are also currently 4 primary hotspots in the Indo-Atlantic box: Iceland, Afar, Kerguelen and Reunion. The number of upwellings, the size of the domes, the spacing between the domes and the primary hotspots and the time recurrence between past traps and present day primary hotspots are consistent with predictions from convection experiments in the case of thermochemical instabilities rising from the first 500 km at the bottom of the mantle.

In the last 260 Myr, only six upwellings in the Indo-Atlantic box had the « balloon on a string » morphology of the classical mantle plume model. All upwellings are transient features. Therefore interpreting present-day tomographic images is delicate. This study is a first attempt but calls for many improvements. We are lacking reliable images of the mantle zone between 400 and 1000 km, so that the connexion between large upwellings in the lower mantle and hot spots and secondary plumes in the upper mantle remains hypothetical. The transition zone also remains enigmatic from a fluid mechanics point of view: it obviously plays a filtering role on the upwellings but more work is needed to understand it quantitatively. To understand the origin of compositional heterogeneities, we would need to distinguish between the relative contributions of temperature, chemistry and partial melt in the tomographic images. Last, in order to reconstruct the past history of convection in the mantle, we now need to fully understand and quantify the influence of doming on true polar wander, which may explain remaining puzzles (such as the proximity in time and space of the Madagascar and Kerguelen traps which would contradict Fig. 6b). Deciphering the convective history of our planet will clearly require increasingly cross-disciplinary studies.

Acknowledgements

This work benefited from discussions with Steve Grand, Barbara Romanowicz, Jeroen Ritsema, Rafaella Montelli, Claude Jaupart, Neil Ribe, Jean-Paul Montagner, Alain Bonneville and Don Helmberger, and from thoughtful reviews from Norm Sleep and an anonymous reviewer. We are grateful to Barbara Romanowicz, Steve Grand and Jeroen Ritsema for

providing their tomographic models. This is IPGP contribution 2091.

Appendix A. Supplementary material

Supplementary data associated with this article can be found, in the online version, at doi:10.1016/j.epsl.2005.07.024.

References

[1] G. Masters, T.H. Jordan, P.G. Silver, F. Gilbert, Aspherical Earth structure from fundamental spheroidal-mode data, Nature 298 (1982) 609–613.
[2] R.D. van der Hilst, S. Widiyantoro, E.R. Engdahl, Evidence for deep mantle circulation from global tomography, Nature 386 (1997) 578–584.
[3] M.A. Richards, D.C. Entgebretson, Large-scale mantle convection and the history of subduction, Nature 355 (1992) 437–440.
[4] M. Gurnis, Large-scale mantle convection and the aggregation and dispersal of supercontinents, Nature 335 (1988) 695–699.
[5] D. Bercovici, The generation of plate tectonics from mantle convection, Earth Planet. Sci. Lett. 205 (2003) 107–121.
[6] Y. Ricard, M.A. Richards, C. Lithgow-Bertelloni, Y. Le Stunff, A geodynamical model of mantle density heterogeneity, J. Geophys. Res. 98 (21) (1993) 895–21909.
[7] C. Lithgow -Bertelloni, M.A. Richards, Cenozoic plate driving forces, Geophys. Res. Lett. 22 (1995) 1317–1320.
[8] M. Gurnis, Phanerozoic marine inundation of continents driven by dynamic topography above subducting slabs, Nature 364 (1993) 589–593.
[9] F.H. Busse, Quadrupole convection in the lower mantle? Geophys. Res. Lett. 10 (1983) 285–288.
[10] M.K. McNutt, K.M. Fisher, The South Pacific superswell, in: B.H. Keating, et al., (Eds.), Seamounts, Islands and Atolls, Geophys. Monogr., vol. 43, AGU, Washington D.C., 1987, pp. 123–132.
[11] A.A. Nyblade, S.W. Robinson, The African superswell, Geophys. Res. Lett. 21 (1994) 765–768.
[12] A. Cazenave, C. Thoraval, Mantle dynamics constrained by degree 6 surface topography, seismic tomography and geoid: inference on the origin of the South Pacific superswell, Earth Planet. Sci. Lett. 122 (1994) 207–219.
[13] C. Lithgow -Bertelloni, P.G. Silver, Dynamic topography, plate driving forces and the African superswell, Nature 395 (1998) 269–272.
[14] J.T. Wilson, Evidence from islands on the spreading of the ocean floor, Can. J. Phys. 41 (1963) 863–868.
[15] G.F. Davies, Ocean bathymetry and mantle convection, 1, large-scale flow and hotspots, J. Geophys. Res. 93 (1988) 10467–10480.
[16] N.H. Sleep, Hotspots and mantle plumes: some phenomenology, J. Geophys. Res. 95 (1990) 6715–6736.
[17] B. Steinberger, Plumes in a convecting mantle: models and observations for individual hotspots, J. Geophys. Res. 105 (2000) 11127–11152.
[18] V. Courtillot, A. Davaille, J. Besse, J. Stock, Three distinct types of hotspots in the Earth's mantle, Earth Planet. Sci. Lett. 205 (2003) 295–308.
[19] W.J. Morgan, Plate motions and deep mantle convection, Nature 230 (1971) 42–43.
[20] M.A. Richards, R.A. Duncan, V.E. Courtillot, Flood basalts and hot-spot tracks: plume heads and tails, Science 246 (1989) 103–107.
[21] R.S. White, D.M. McKenzie, Magmatism at rift zones: the generation of volcanic continental margins and flood basalts, J. Geophys. Res. 94 (1989) 7685–7729.
[22] K.A. Farley, E. Naroda, Noble gases in the Earth's mantle, Annu. Rev. Earth Planet. Sci. 26 (1998) 189–218.
[23] M. Gurnis, J.X. Mitrovica, J. Ritsema, H.-J. van Heijst, Constraining mantle density structure using geological evidence of surface uplift rates: the case of the African superplume, Geochem. Geophys. Geosyst. 1 (2000), doi:10.1029/1999GC000035.
[24] A.M. Dziewonski, D.L. Anderson, Preliminary reference Earth model, Phys. Earth Planet. Inter. 25 (1981) 297–356.
[25] G. Masters, G. Laske, F. Gilbert, Large-scale Earth structure from analyses of free-oscillation splitting and coupling, in: E. Boschi, G. Ekstroem, A. Morelli (Eds.), Problems in Geophysics for the New Millenium, Instituto Nazionale di Geofisica e Vulcanologia, Rome, Italy, 2000, pp. 255–288.
[26] S. Karato, Importance of anelasticity in the interpretation of seismic tomography, Geophys. Res. Lett. 20 (1993) 1623–1626.
[27] J. Trampert, F. Deschamps, J. Resovsky, D. Yuen, Probalistic tomography maps chemical heterogeneity throughout the lower mantle, Science 306 (2004) 853–856.
[28] B. Romanowicz, Global mantle tomography: progress status in the last 10 years, Annu. Rev. Geoph. Space Phys. 31 (2003) 303.
[29] S.P. Grand, R.D. van der Hilst, S. Widiyantoro, Global seismic tomography: a snapshot of convection in the earth, GSA Today 4 (1997) 1–7.
[30] C. Mégnin, B. Romanowicz, A model of shear velocity in the mantle from the inversion of waveforms of body, surface and higher mode waveforms, Geophys. J. Int. 143 (2000) 709.
[31] J. Ritsema, H.J. van Heijst, Seismic imaging of structural heterogeneity in Earth's mantle: evidence for large-scale mantle flow, Sci. Prog. 83 (2000) 243–259.
[32] J. Ritsema, S. Ni, D.V. Helmberger, H.P. Crotwell, Evidence for strong shear velocity reductions and velocity gradients in the lower mantle beneath Africa, Geophys. Res. Lett. 25 (1998) 4245–4248.
[33] S. Ni, E. Tan, M. Gurnis, D. Helmberger, Sharp sides to the African superplume, Science 296 (2002) 1850–1852.
[34] S. Ni, D. Helmberger, Seismological constraints on the South African superplume: could be the oldest distinct structure on Earth, Earth Planet. Sci. Lett. 206 (2003) 119–131.

[35] G. Silveira, E. Stutzmann, Anisotropic tomography of the Atlantic Ocean, Phys. Earth Planet. Inter. 132 (2002) 237–248.
[36] C.J. Wolfe, I.T. Bjarnason, J.C. VanDecar, S.C. Solomon, Seismic structure of the Iceland mantle plume, Nature (1997) 245–247.
[37] E. Debayle, J.J. Lévêque, M. Cara, Seismic evidence for a deeply rooted low velocity anomaly in the upper mantle beneath the northeastern Afro/Arabian continent, Earth Planet. Sci. Lett. 193/3–4 (2001) 369–382.
[38] R. Montelli, G. Nolet, F.A. Dahlen, G. Masters, E.R. Engdahl, S.-H. Hung, Finite-frequency tomography reveals a variety of plumes in the mantle, Science 303 (2004) 338–343.
[39] V. Courtillot, P.R. Renne, On the ages of flood basalt events, CRAS Géosci. 335/1 (2003).
[40] A. Marzoli, P.R. Renne, E.M. Piccirillo, M. Ernesto, G. Bellieni, A. De Min, Extensive 200-Million-year-old continental flood basalts of the Central Atlantic Magmatic Province, Science 284 (1999) 616–618.
[41] B.C. Storey, The role of mantle plumes in continental break up: case histories from Gondwanaland, Nature 377 (1995) 301–308.
[42] R.S. White, D.M. McKenzie, Mantle plumes and flood basalts, J. Geophys. Res. 100 (1995) 17543–17585.
[43] R.C.O. Gill, A.K. Pedersen, J.G. Larsen, Tertiary picrites in West Greenland: melting at the periphery of a plume? in: S.A. Storey, Alabaster, Pankhurst (Eds.), Magmatism and the Causes of Continental Break-Up, Geol. Soc. Spec. Pub., vol. 68, 1992, pp. 335–348.
[44] R.N. Thompson, S.A. Gibson, Transient high temperatures in mantle plume heads inferred from magnesian olivines in Phanerozoic picrites, Nature 407 (2000) 502–505.
[45] M. Schimmel, M. Assumpção, J. Vandecar, Upper mantle seismic velocity structure beneath SE Brazil from P- and S-wave travel time inversions, J. Geophys. Res. 108 (2003) 2191, doi:10.1029/2001 JB000187.
[46] B.L.N. Kennett, S. Widyantoro, A low seismic wavespeed anomaly beneath northwestern India: a seismic signature of the Deccan plume? Earth Planet. Sci. Lett. 165 (1999) 145–155.
[47] L. Vinnik, V. Farra, Subcratonic low-velocity layer and flood basalts, Geophys. Res. Lett. 29 (2002), doi:10.1029/2001GL014064.
[48] K. Burke, T.H. Torsvik, Derivation of large igneous provinces of the past 200 Myr from long-term heterogeneities in the deep mantle, Earth Planet. Sci. Lett. 227 (2004) 531–538.
[49] D.L. Anderson, Hotspots, polar wander, Mezosoic convection and the geoid, Nature 297 (1982) 391–393.
[50] M. Wilson M., Magmatism and continental rifting during the opening of the South Atlantic Ocean: a consequence of lower Cretaceaous super-plume activity? in: D.S. Storey, Alabaster, Pankhurst (Eds.), Magmatism and the Causes of Contiental Break-Up, Geol. Soc. Spec. Pub., vol. 68, 1992, pp. 241–255.
[51] J.A. Whitehead, D.S. Luther, Dynamics of laboratory diapir and plume models, J. Geophys. Res. 80 (1975) 705–717.
[52] P. Olson, H. Singer, Creeping plumes, J. Fluid Mech. 158 (1985) 511–531.
[53] R.W. Griffiths, I.H. Campbell I.H., Stirring and structure in mantle starting plumes, Earth Planet. Sci. Lett. 99 (1990) 66–78.
[54] H.-C. Nataf, Mantle convection, plates, and hotspots, Tectonophysics 187 (1991) 361–371.
[55] G. Schubert, G. Masters, P. Olson, P. Tackley, Superplumes or plume clusters? Phys. Earth Planet. Inter. 146 (2004) 147–162.
[56] Q. Williams, The temperature contrast across D″, The Core–Mantle Boundary Region, AGU Monogr., 1998, pp. 73–81.
[57] A. Davaille, F. Girard, M. Le Bars, How to anchor hotspots in a convecting mantle? Earth Planet. Sci. Lett. 203 (2002) 621–634.
[58] P. Olson, An experimental approach to thermal convection in a two-layered mantle, J. Geophys. Res. 89 (1984) 11293–11301.
[59] A. Davaille, Simultaneous generation of hotspots and superswells by convection in a heterogeneous planetary mantle, Nature 402 (1999) 756–760.
[60] D.L. Herrick, E.M. Parmentier, Episodic large-scale overturn of two-layer mantles in terrestrial planets, J. Geophys. Res. 99 (1994) 2053–2062.
[61] M. LeBars, A. Davaille, Large interface deformation in two-layer thermal convection of miscible viscous fluids, J. Fluid Mech. 499 (2004) 75–110.
[62] M. LeBars, A. Davaille, Whole-layer convection in an heterogeneous planetary mantle, J. Geophys. Res. 109 (2004), doi:10.1029/2003JB002617.
[63] P.F. Thompson, P.J. Tackley, Generation of mega-plumes from the core-mantle boundary in a compressible mantle with temperature-dependent viscosity, Geophys. Res. Lett. 25 (1998) 1999–2002.
[64] U. Christensen, Instability in a hot boundary layer and initiation of thermo-chemical plumes, Ann. Geophys. 2 (1984) 311–320.
[65] G.C. Farnetani, Excess temperature of mantle plumes: the role of chemical stratification across D″, Geophys. Res. Lett. 24 (1997) 1583–1586.
[66] P.J. Tackley, Three-dimensional simulations of mantle convection with a thermo-chemical basal boundary layer: D″? The Core–Mantle Boundary Region, AGU Monogr., 1998, pp. 231–253.
[67] A. Davaille, Two-layer thermal convection in miscible viscous fluids, J. Fluid Mech. 379 (1999) 223–253.
[68] A. Namiki, K. Kurita, The influence of boundary heterogeneity in experimental models of mantle convection, Geophys. Res. Lett. 26 (1999) 1929–1932.
[69] A.M. Jellineck, M. Manga, Links between long-lived hotspots, mantle plumes, D″, and plate tectonics, Rev. Geophys. 42 (2004), doi:10.1029/2003RG000144.
[70] P.J. Tackley, On the penetration of an endothermic phase transition by upwellings and downwellings, J. Geophys. Res. 100 (1996) 15477–15488.
[71] L. Cserepes, D. Yuen, On the possibility of a second kind of mantle plume, Earth Planet. Sci. Lett. 183 (2000) 61–71.
[72] H.-C. Nataf, C. Froidevaux, J.L. Levrat, M. Rabinowicz, Laboratory convection experiments: effect of lateral cooling

and generation of instabilities in the horizontal boundary layers, J. Geophys. Res. 86 (1981) 6143–6154.
[73] A.M. Jellineck, H.M. Gonnermann, M.A. Richards, Plume capture by divergent plate motions: implications for the distribution of hotpsots, geochemistry of mid-ocean ridge basalts, and estimates of the heat flux at the core–mantle boundary, Earth Planet. Sci. Lett. 205 (2003) 361–378.
[74] H.M. Gonnermann, A.M. Jellinek, M.A. Richards, M. Manga, Modulation of mantle plumes and heat flow at the core mantle boundary by plate-scale flow: results from laboratory experiments, Earth Planet. Sci. Lett. 226 (2004) 53–67.
[75] J.P. Lowman, S.D. King, C.W. Gable, Steady plumes in viscously stratified, vigorously convecting, three-dimensinoal numerical mantle convection models with mobile plates, Goechem. Geophys. Geosyst. 5 (2004), doi:10.1029/2003GC000583.
[76] S.D. King, J. Ritsema, African hot spot volcanism: small-scale convection in the upper mantle beneath cratons, Science 290 (2000) 1137–1140.
[77] J. Besse, V. Courtillot, Revised and synthetic apparent polar wander paths of the African, Eurasian, North American and Indian plates, and true polar wander since 200 Ma, J. Geophys. Res. 96 (1991) 4029–4050.
[78] J. Besse, V. Courtillot, Apparent and true polar wander and the geometry of the geomagnetic field over the last 200 Myr, J. Geophys. Res. 107 (B11) (2002) 2300, doi:10.1029/2000JB000050.
[79] X. Zhao, R.S. Coe, S.A. Gilder, G.M. Frost, Palaeomagnetic constraints on the palaeogeography of China: implications for Gondwanaland, Aust. J. Earth Sci. 43 (1996) 643–672.
[80] J. Besse, F. Torcq, Y. Gallet, L.E. Ricou, L. Krystyn, A. Saidi, Late Permian to Late Triassic palaeomagnetic data from Iran: constraints on the migration of the Iranian block through the Tethyan ocean and initial destruction of Pangaea, Geophys. J. Int. 135 (1998) 77–92.
[81] N. Halim, J.P. Cogne, Y. Chen, R. Atasiei, J. Besse, V. Courtillot, S. Gilder, J. Marcoux, R.L. Zhao, New cretaceous and early tertiary paleomagnetic results from Xining-Lanzhou Basin, Kunlun and Qiangtang blocks, China: implications on the geodynamic evolution of Asia, J. Geophys. Res. 103 (1998) 21025–21045.
[82] Yang, J. Besse, New mesozoic apparent polar wandering path for South China: tectonic consequences, J. Geophys. Res. 106 (2001) 8493–8520.
[83] F. Fluteau, J. Besse, J. Broutin, M. Berthelin, Extension of Cathaysian flora during the Permian — Climatic and paleogeographic constraints, Earth Planet. Sci. Lett. 193 (3–4) (2001) 603–616.
[84] J.P. Cogné, PaleoMac: a Macintosh™ application for treating paleomagnetic data and making plate reconstructions, Geochem. Geophys. Geosyst. 4 (2003) 1007, doi:10.1029/2001GC000227.
[85] F.M. Richter, D.P. McKenzie, On some consequences and possible causes of layered convection, J. Geophys. Res. 86 (1981) 6124–6133.
[86] P. Olson, C. Kincaid, Experiments on the interaction of thermal convection and compositional layering at the base of the mantle, J. Geophys. Res. 96 (1991) 4347–4354.
[87] H. Schmeling, Numerical models of Rayleigh-Taylor instabilities superimposed upon convection, Bull. Geol. Inst. Univ. Upps. 14 (1988) 95–109.
[88] L.H. Kellogg, B.H. Hager, R.D. van der Hilst, Compositional stratification in the deep mantle, Science 283 (1999) 1881–1884.
[89] N.L. Montague, L.H. Kellogg, Numerical models of a dense layer at the base of the mantle and implications for the geodynamics of D″, J. Geophys. Res. 105 (2000) 11101–11114.
[90] U. Hansen, D.A. Yuen, Extended-Boussinesq thermal-chemical convection with moving heat sources and variable viscosity, Earth Planet. Sci. Lett. 176 (2000) 401–411.
[91] H. Samuel, C.G. Farnetani, Thermochemical convection and helium concentrations in mantle plumes, Earth Planet. Sci. Lett. 207 (2002) 39–56.
[92] A.K. McNamara, S. Zhong, Thermochemical structures within a spherical mantle: superplumes or piles? J. Geophys. Res. 109 (2004), doi:10.1029/2003JB002847.